Statistical Evaluation of Delay and Doppler Spread in 60 GHz Vehicle-to-Vehicle Channels During Overtaking

E. Zöchmann[*†] M. Hofer[‡] M. Lerch[†] J. Blumenstein[§] S. Sangodoyin[¶]
H. Groll[†] S. Pratschner[*†] S. Caban[†] D. Löschenbrand[‡] L. Bernadó[‡]
T. Zemen[‡] A. Prokes[§] M. Rupp[†] C. F. Mecklenbräuker[†] A. F. Molisch[¶]

***Abstract* — Millimeter waves experience much higher maximum Doppler shifts than their centimeter wave counterparts. We measured the wireless channel of 36 different overtaking vehicles to obtain delay and Doppler spread values based on ensemble averages. Our TX antenna is a horn with an 18 degree half power beam width. Spatial filtering by this narrow beam decreases the delay and Doppler spread values. We observe that the RMS Doppler spread is effectively below one-tenth of the maximum Doppler shift. For example, at 60 GHz a relative speed of 30 km/h yields a maximum Doppler shift of approximately 3.3 kHz and a median RMS Doppler spread of 220 Hz at the utmost. The largest median RMS delay spread observed is 5.3 ns.**

1 INTRODUCTION

Today, automated urban metro subway systems are operating in more than sixty cities around the globe proving that driverless transportation systems are fully accepted by the public. Although introducing many novel degrees of freedom, automated driverless road systems are emerging with the expectation to drastically reduce the number of fatal crashes together with an increased comfort of utilization. Safety and reliability of the driverless road systems are not only determined by the performance of the sensor equipment (see e.g. [1]). An irreplaceable role has vehicular wireless communications for safety critical message exchange. Because of the current improvements in the technology of integrated circuits, broadband vehicular millimeter-wave (mmW) communications has gained interest [2]. Similarly as for the railroad case [3], vehicle-to-vehicle (V2V) and vehicle-to-infrastructure (V2I) wireless channels, determining the performance and reliability of the communication links, need to be thoroughly understood and characterized at mmW frequencies. Millimeter wave vehicular communications has two main distinctive features as compared to sub-6-GHz vehicular communications; firstly, the use of directive antennas (at least at one link end) and secondly, the much higher maximum Doppler shift [4]. Pioneering work has been performed by [5], where the performance of 60 GHz V2V wireless links has been measured. In [6], V2V channel measurements at 38 GHz and 60 GHz, using a channel sounder with 1 GHz bandwidth, have been conducted. In [7], V2V large-scale fading and small-scale fading analysis is provided for 73 GHz. Intra-vehicular Doppler spectra of vibrations appearing while the vehicle is in operation are shown in [8].

Our contribution: In this paper we characterize the typical delay-Doppler spreads occurring during an overtaking maneuver while distinguishing two classes, represented by (1) passenger cars and sport utility vehicles (SUVs) and (2) trucks and buses.

2 MEASUREMENT SETUP

We measured a set of vehicle-to-vehicle channel realizations to capture the effect of an overtaking vehicle. The measurement data evaluated for this contribution consists of 36 different vehicular channels. By using a directive antenna at the TX — through *spatial filtering* — Doppler is mainly determined by the relative velocity of the overtaking vehicle, that is, the excess speed of the overtaking vehicle. Hence, we keep the TX and RX static and in channel sounding mode while other vehicles from the ordinary street traffic pass by.

Our measurement setup has been introduced in detail in [9]. For a sketch of the setup see Fig. 1. A photograph of the whole setup is shown in Fig. 3. A measurement is triggered once the overtaking vehicle is driving through a first light barrier. The mean velocity of the vehicle is estimated through a second light barrier. Memory space is limiting the record length of our 500 MHz broadband signal to 720 ms. Due to this limitation, the recorded measurements covered less than 12 m. To cover the distance shown in Fig. 1, the light barriers, triggering the measurements, are placed at three different positions.

[*]Christian Doppler Laboratory for Dependable Wireless Connectivity for the Society in Motion, Institute of Telecommunications, TU Wien, Austria ezoechma@nt.tuwien.ac.at
[†]Institute of Telecommunications, TU Wien, Austria
[‡]Center for Digital Safety & Security, AIT Austrian Institute of Technology, Austria
[§]Department of Radio Electronics, TU Brno, Czech Republic
[¶]Wireless Devices and Systems Group, University of Southern California, USA

3 DATA POST-PROCESSING

For the statistical evaluation of the measurement data, we firstly cluster the vehicles into two groups. Smaller vehicles such as cars and SUVs are referred to as "cars" and larger vehicles such as trucks and buses are referred to as "trucks" in the sequel. Secondly, we calculate the position of the overtaking vehicle as a function of the first light barrier's placement and the light barrier based estimate of the mean speed. Thirdly, we calculate the local scattering function (LSF), see [9] and the references therein, as a function of record time (estimated distance). The stationarity length is set to 15 ms. Fourthly, the LSF is noise-thresholded. The median of all samples of the LSF is used as threshold. As most samples of the LSF consist of noise, the median is a good estimator for the noise power in a sparse channel [10]. Fifthly, to obtain the power delay profile (PDP) and the Doppler spectral density (DSD) the LSF is marginalized. Sixthly, we estimate the RMS delay spread σ_τ and the RMS Doppler spread σ_ν as in [11]. To compare vehicles with different speed, the Doppler profile of each vehicle is first normalized w.r.t. to its maximum Doppler shift $\nu_{\max} = {}^{2v}/_{\lambda}$. Next the Doppler profile is re-scaled to a common speed of $v = 30\,{}^{\mathrm{km}}/_{\mathrm{h}} \approx 8.33\,{}^{\mathrm{m}}/_{\mathrm{s}}$. Lastly, to increase robustness, we calculate the mean delay spread and mean Doppler spread for each vehicle within one meter. The data post-processing for one exemplary vehicle is shown in Fig. 2. The results for the whole data ensemble are illustrated via box plots in Fig. 4, with 25^{th} and 75^{th} percentiles indicated. The third subplot shows the number of collected snapshots used for the evaluation at each individual position.

4 DISCUSSION AND CONCLUSION

The RMS delay spread, illustrated in the top part of Fig. 4, is only slightly affected by an overtaking vehicle. The horn antenna at the TX is aligned to the line-of-sight (LOS) towards the RX antenna. LOS is unblocked and dominates all other multipath components (MPCs). If a truck is close to the RX antenna (at approx. 1 m to 2 m) it shadows the background and σ_τ is the least. After 4 m, due to its bigger rear surface, trucks generate MPCs that increase σ_τ slightly. Cars barely alter σ_τ. The RMS Doppler spread of cars at distances close to the antenna (< 4 m) is mainly due to phase noise of our equipment. Cars show the strongest effect on σ_ν at approx. 7 to 8 meters. There, geometrically the Doppler shift is already close to $\nu_{\max}$ and the object is still close enough to appear as strong MPC. At larger distances the MPC belonging to the overtaking car fades out. Note the similarity of σ_ν for cars and trucks after 7 m. In this region only the rear part of the vehicles is illuminated. On the other hand, if a truck is near the RX antenna, the entire side wall produces very strong MPCs. This cluster of MPCs increases σ_ν significantly.

Conclusion: Due to the spatial filtering of the horn antenna, the RMS Doppler spread is less than 12% of the maximum Doppler shift ($\sigma_\nu \leq 0.12\,\nu_{\max}$). For comparison, a Doppler shift uniformly distributed in $(-\nu_{\max}, 0)$ yields $\sigma_\nu = {}^{\nu_{\max}}/_{\sqrt{12}} \approx 0.3\,\nu_{\max}$, a Doppler shift distributed according to a half-Jakes' density yields $\sigma_\nu = \nu_{\max}\sqrt{{}^{(\pi^2-2^2)}/_{(2\pi)^2}} \approx 0.4\,\nu_{\max}$, and a Doppler shifted according to a Jakes' density even $\sigma_\nu = {}^{\nu_{\max}}/_{\sqrt{2}} \approx 0.7\,\nu_{\max}$. Modeling σ_ν with these models is therefore not appropriate. Furthermore, since the maximum observed σ_ν is only four times stronger than the phase noise of our system, our vehicular mmW "overtaking" channel is not much more challenging than static indoor channels.

Acknowledgments

The financial support by the Austrian Federal Ministry of Science, Research and Economy and the National Foundation for Research, Technology and Development is gratefully acknowledged. The research described in this paper was co-financed by the Czech Science Foundation, Project No. 17-27068S and 17-18675S, and by National Sustainability Program under grant LO1401. For the research, the infrastructure of the SIX Center was used. The work of S. Sangodoin and A. F. Molisch was supported by the NSF and NIST. This work was carried out in the framework of COST Action CA15104 IRACON.

References

[1] T. Tokumitsu, M. Kubota, K. Sakai, and T. Kawai, "Application of GaAs device technology to millimeter-waves," *SEI Technical Review*, no. 79, pp. 57–65, 2014.

[2] V. Va, T. Shimizu, G. Bansal, and R. W. Heath Jr, "Millimeter wave vehicular communications: A survey," *Foundations and Trends® in Networking*, vol. 10, no. 1, pp. 1–113, 2016.

[3] H. Meinel and A. Plattner, "Millimetre-wave propagation along railway lines," *IEE Proceedings F (Communications, Radar and Signal Processing)*, vol. 130, no. 7, pp. 688–694, 1983.

[4] E. Zöchmann, S. Caban, M. Lerch, and M. Rupp, "Resolving the angular profile of 60 GHz wireless channels by delay-Doppler measurements," in *Proc. of IEEE Sensor Array and Multichannel Signal Processing Workshop (SAM)*, 2016, pp. 1–5.

[5] A. Kato, K. Sato, M. Fujise, and S. Kawakami, "Propagation characteristics of 60-GHz millimeter waves for ITS inter-vehicle communications," *IEICE Transactions on Communications*, vol. 84, no. 9, pp. 2530–2539, 2001.

[6] M. G. Sánchez, M. P. Táboas, and E. L. Cid, "Millimeter wave radio channel characterization for 5G vehicle-to-vehicle communications," *Measurement*, vol. 95, pp. 223–229, 2017.

[7] H. Wang, X. Yin, X. Cai, H. Wang, Z. Yu, and J. Lee, "Fading characterization of 73 GHz millimeter-wave V2V channel based on real measurements," *Communication Technologies for Vehicles*, p. 159, 2018.

[8] A. Prokes, J. Vychodil, M. Pospisil, J. Blumenstein, T. Mikulasek, and A. Chandra, "Time-domain non-

stationary intra-car channel measurement in 60 GHz band," in *2016 International Conference on Advanced Technologies for Communications (ATC)*, 2016.

[9] E. Zöchmann *et al.*, "Measured delay and Doppler profiles of overtaking vehicles at 60 GHz," in *Proc. of the 12th European Conference on Antennas and Propagation (EuCAP)*, 2018, pp. 1–5.

[10] E. S. Sousa, V. M. Jovanovic, and C. Daigneault, "Delay spread measurements for the digital cellular channel in Toronto," *IEEE Transactions on Vehicular Technology*, vol. 43, no. 4, pp. 837–847, 1994.

[11] L. Bernadó *et al.*, "Delay and Doppler spreads of non-stationary vehicular channels for safety-relevant scenarios," *IEEE Transactions on Vehicular Technology*, vol. 63, no. 1, pp. 82–93, 2014.

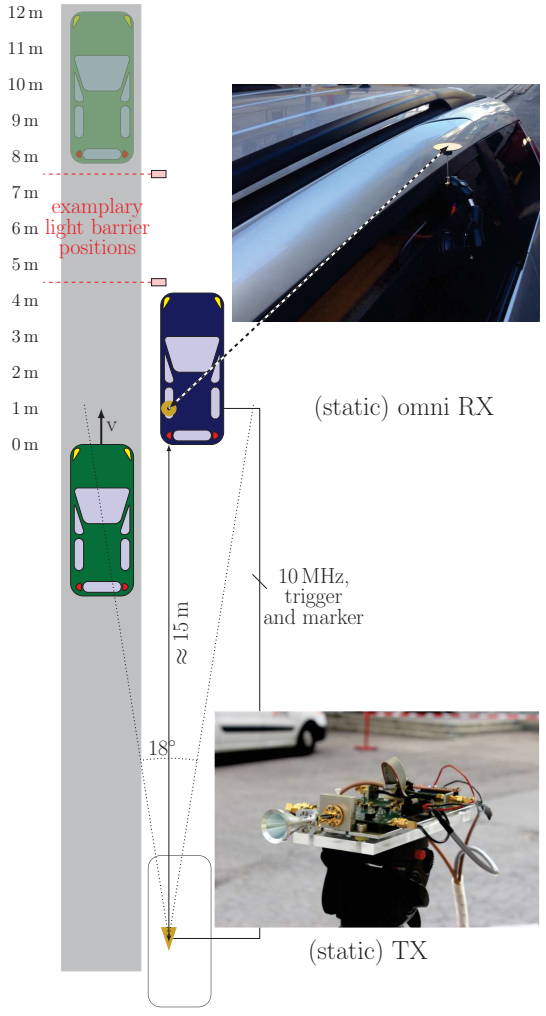

Figure 1: Measurement setup. A conical horn antenna with 18° half power beam width is used at the TX. The RX antenna is a $\lambda/4$ monopole antenna. TX and RX are co-polarized. Our data is plotted against the "front bumper of the overtaking vehicle to the rear bumper of the static RX car" distance. This distance is indicated with meter marks.

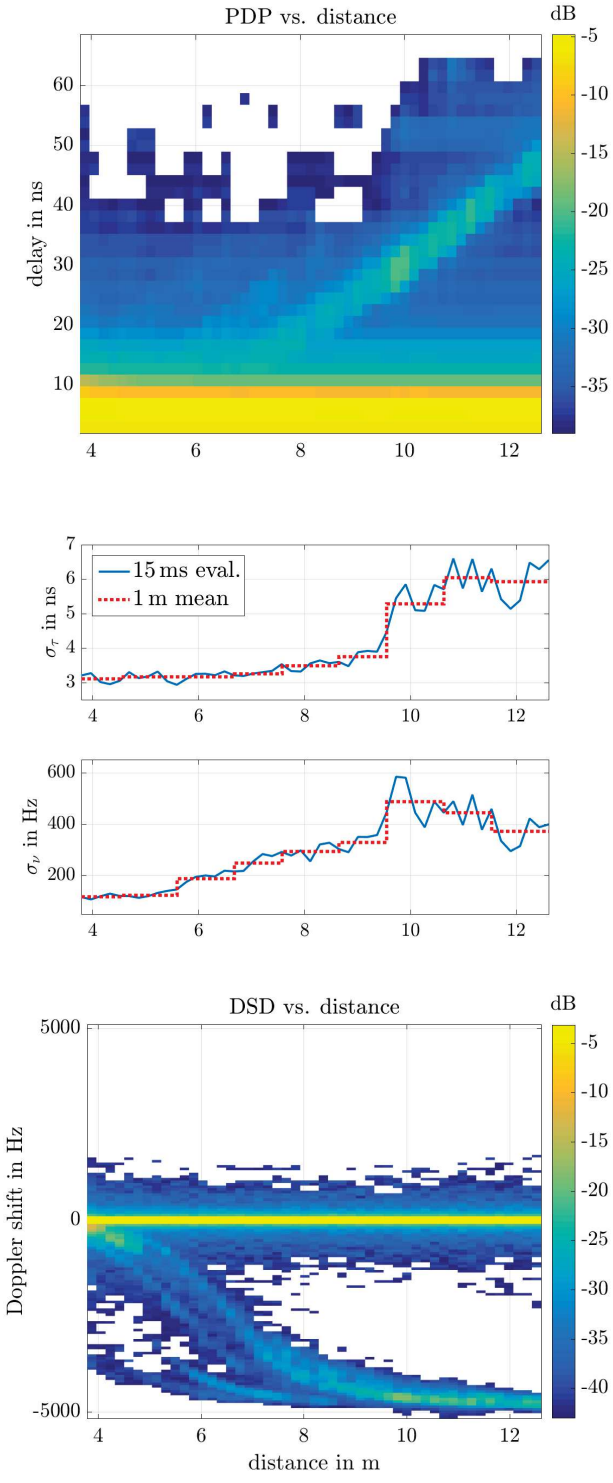

Figure 2: Data post processing example. Lightbarrier placement as indicated in Fig. 1. The overtaking vehicle is a car at a speed of 12 m/s. (top) Estimated PDP after LOS time-alignment and noise thresholding. (middle) Estimated RMS delay spread and estimated RMS Doppler spread. The statistical evaluation is based on the 1 m-averaged results (red dashed line). (bottom) Estimated DSD after noise thresholding.

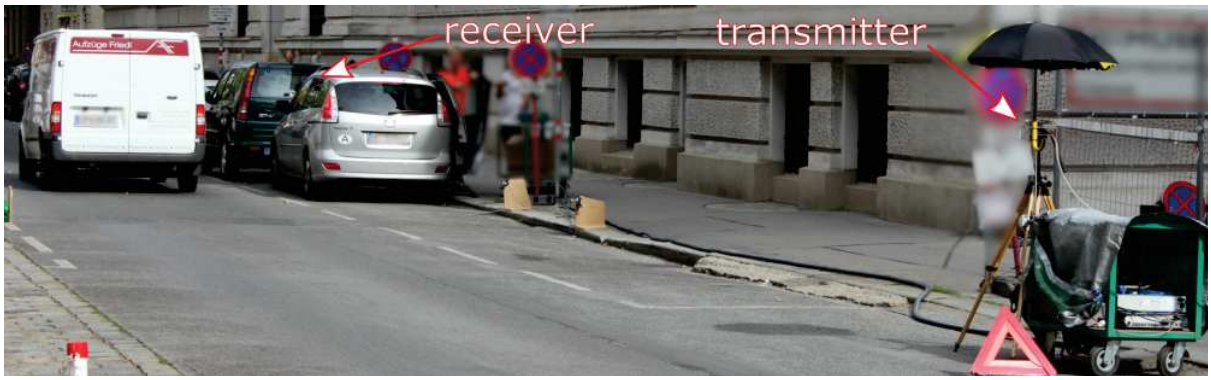

Figure 3: Measurement site. Both TX and RX are static and ordinary street traffic is passing by.

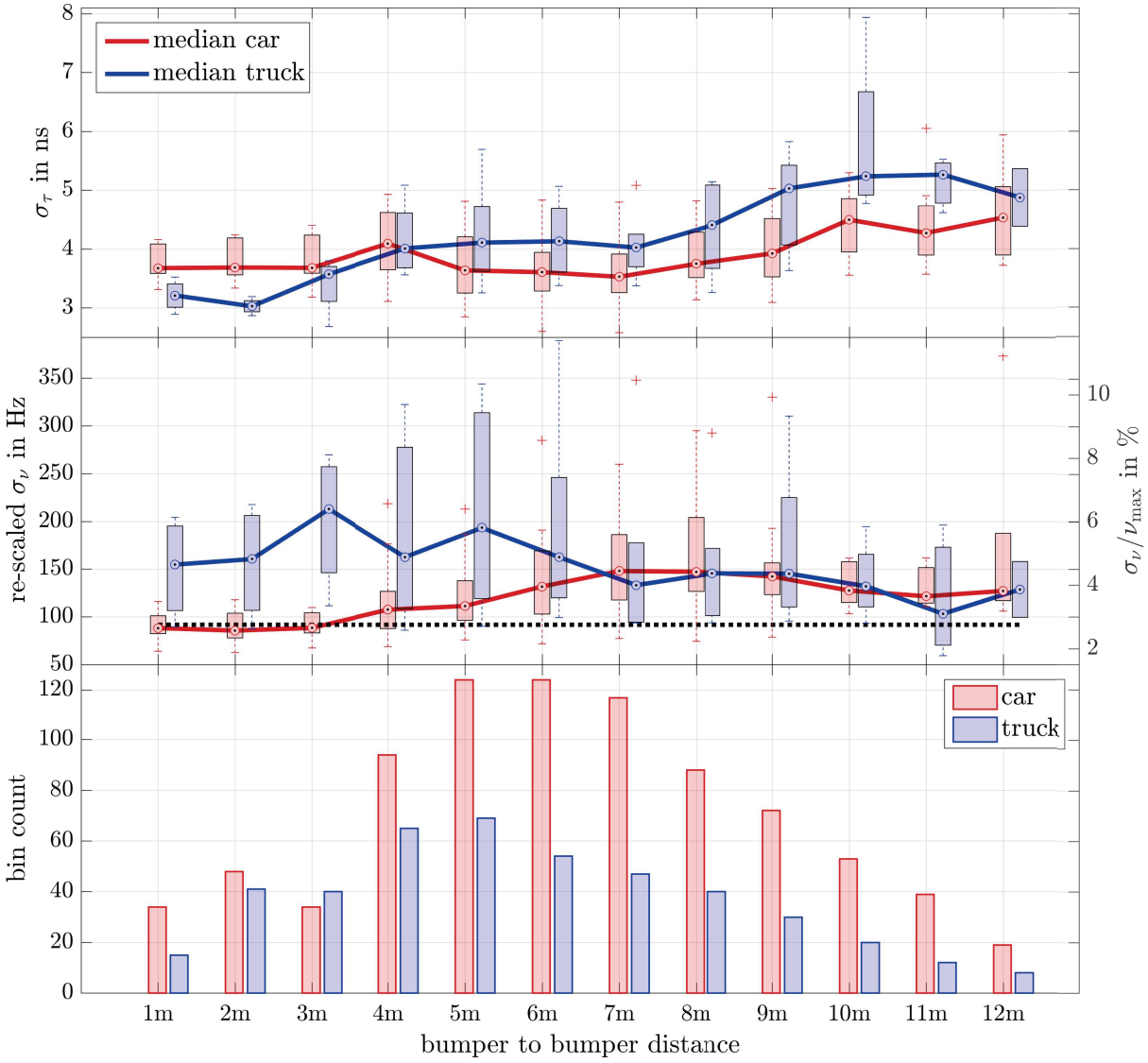

Figure 4: (top) Box plots of RMS delay spread as a function of bumper to bumper distance distinguished by vehicle type. (middle) Box plots of RMS Doppler spread re-scaled to a common vehicle speed of 30 km/h at the left axis and RMS Doppler spread normalized to the maximum Doppler shift at the right axis. The black dotted line shows the estimate for the RMS Doppler spread obtained through the phase noise of our measurement system. (bottom) histogram of channel samples for 15 ms sample lengths.